DYNAMIC MODEL OF A HOT WATER BOILER

Andrei TERNOVEANU and Philippe NGENDAKUMANA

Laboratory of Thermodynamics - University of Liège - Belgium

ABSTRACT

Most of the dynamic models of hot water boilers are either "reference" models or too simplified ones. The formers require sophisticated computation facilities (they are CPU - time consumers) and very detailed data on boiler geometry which are usually not available. The latters are generally identified models based on experimental tests, thus their range of validity is limited to the domain covered by the experimental data.

This paper presents a simplified second order dynamic model which uses available manufacturer data. The model's parameters are adjusted using physical assumptions which take into account real influences as water and flue gas circulation through the boiler. All the parameters defined are physically meaningful.

A special attention is payed to the fast transient short periods (start-up and cut-down) due to their importance for pollutants emission (especially CO). The scope is to provide a flexible model according to the manufacturer data available : the boiler thermal efficiency or the pollutants emission can be predicted.

The results of the model thus built compare well with data obtained on a fuel-oil boiler whose useful power goes up to about 400 kW.

1. INTRODUCTION

Most of the dynamic models of hot water boilers are either "reference" models or too simplified ones. The formers require sophisticated computation facilities (they are CPU - time consumers) and very detailed data on boiler geometry which are usually not available. The latters are generally identified models based on experimental tests, thus their range of validity is limited to the domain covered by the experimental data.

This work deals with the transient behaviour of hot water boilers, and aims at predicting water and flue gas temperature evolutions over cycling regimes of a boiler.The challenge is to develop a dynamic model using essentially available manufacturer data.The model will be focused on the transient short periods (start-up and cool-down) due to their importance for pollutants emission.

2.GENERAL ASSUMPTIONS AND DATA BASE

2.1.The Boiler used for the Model's Validation

The example used is a steel-made, two-block boiler (combustion chamber and heat exchanger). It is fitted with a fuel-oil, two firing-rates burner (on-off control).
The boiler power range is from 200 to 400 kW.
The water and flue gas circuits of the boiler are presented in figure 1.
The structure, dimensions and characteristics are available from producer data.
Concerning the heat losses to the environment, the boiler studied is a particular case, since the lateral side of the combustion chamber is equipped with three quartz windows (for flame visualization).
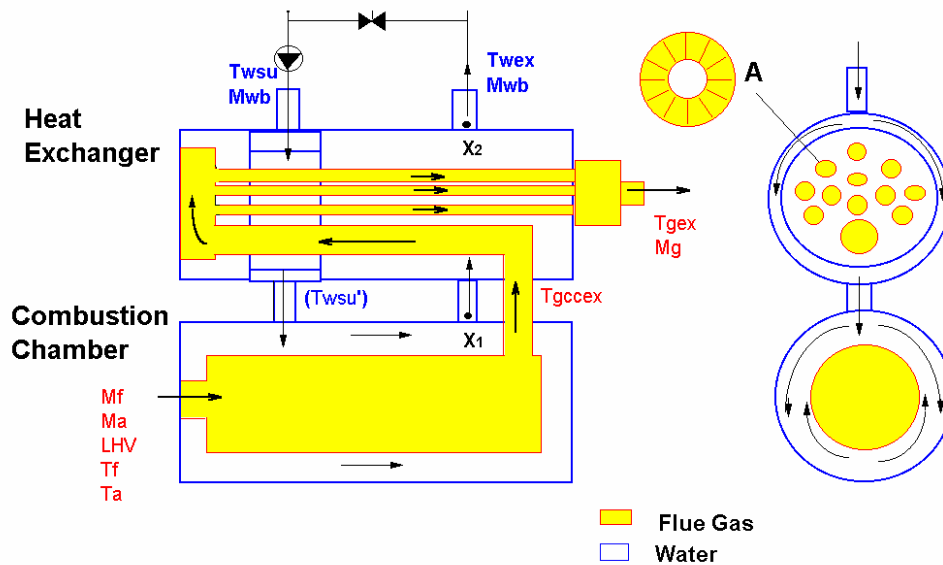
Figure 1. Boiler flue gas and water circuits

2.2.Experimental Data

The results of two start-up tests and one cool-down test are used in the development of the model. Five other tests are used to check the typical temperatures evolutions over the start-up and cool-down periods.

3.THERMAL CAPACITY CALCULATION

The boiler thermal capacity is estimated by means of the materials characteristics, water using the material characteristics, water capacity and metal mass.
Moreover, the data available allow a separate calculation for the combustion chamber and heat exchanger respectively.
The results thus obtained are gathered in Table 1.

The value of the heat exchanger water volume may be split into two values, corresponding to the two circuits as shown in figure 1.
Notice that in the above estimation insulation thermal mass is neglected.

		Comb.ch.	H. Exch.	Total
Metal mass	(kg)	323	656	976
Water volume	$(10^{-3} m^3)$	237	483	720
Thermal capacity	$(10^6$ J/K)	1,142	2,326	3,468

Table 1 : Thermal capacity values

4.SIMULATION OF "START-UP" REGIME

4.1.Introduction

The transient behaviour of the studied boiler over the "start-up" regime is simulated using two different models corresponding to two cases of typical assumptions.
Predicted water and flue gas temperature evolutions are compared with the experimental results.

4.2. Stabilization Period

Iorder to choose the stabilization period, the accuracy of the experimental results is taken into account. It is assumed that the error on the useful power due to stabilization time must not exceed that due to the measurements accuracy :

$$ e^{-\frac{\tau_s}{\tau_c}} \leq \varepsilon_m \tag{1} $$

where : τ_c , τ_s are the boilers time constant and the stabilization time respectively (sec).
ε_m is the mean relative error on the useful power.
The value corresponding to the errors range observed in previous tests is : $\tau_s = 5,5 \ \tau_c$

4.3.The Experimental Results

The results of two "heat-up" tests at low (LFR) and high firing rates(HFR) are available.
The values corresponding to steady-state regimes are given in table 2.

Test number	Firing rate	$\dot{M}_{wc}$ 2	$\dot{M}_{fuel}$ 3	Tw_c (°C)	Tw_{ex} (°C)	Tw_{su} (°C)	Tg_{ex} (°C)	Tg_{ccex} (°C)	$1 + e$

3

		(kg/s)	(kg/s)						
1115	HFR	1.301	9,71 10^{-3}	11,8	80,8	60,3	197	945	1,10
0223	LFR	0,693	5,58 10^{-3}	8,5	84,3	70,9	152	848	1,20

**Table 2 : Synthesis of Experimental Results - Steady-state Values**

The typical evolution of water and flue gas temperatures is shown in figure 2. Notice that the start-up is characterized by two distinct periods.

The first one corresponds to a fast stabilization of flue gas temperature at combustion chamber exhaust and to a "dead" time (τ_o) on water exhaust temperature (transport time to the boiler exhaust).

The second period presents classic transient shapes for exhaust temperatures .

Note :1) As the measure time step is 20 sec., the fast transient period is not studied accurately;

2) The water/gas ratio on flow-time across the boiler is estimated at about 10^2.It corresponds to an instantaneous response on flue gas and a delayed one on water side.
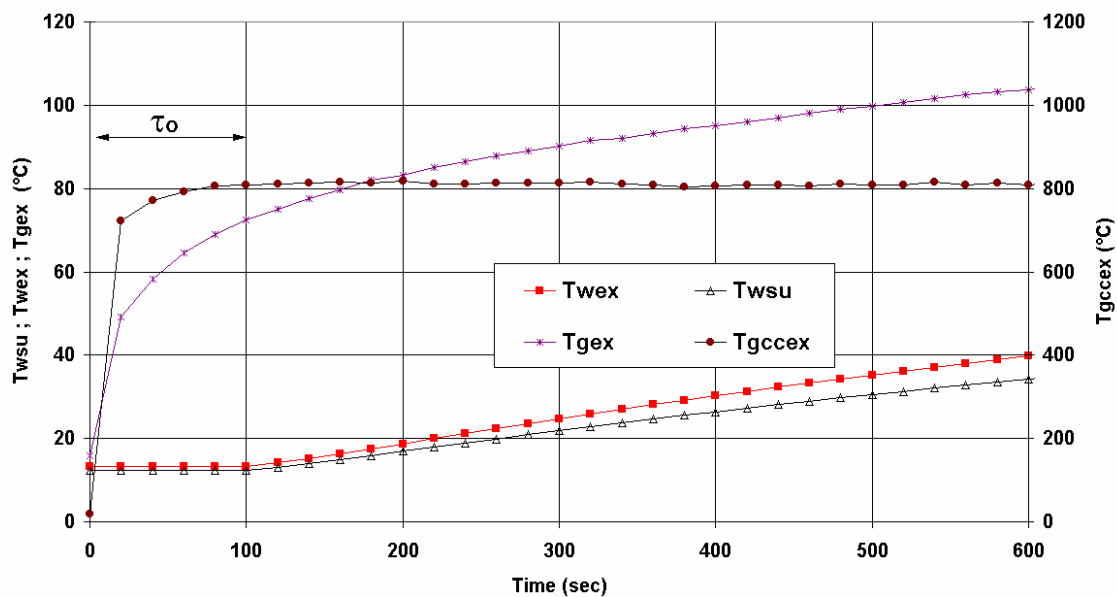
Figure 2. Typical evolutions of the flue gas and water temperatures

4.4.Typical Assumptions - First Modelling Case

The following assumptions are made for a first modelling of the start-up regime :

1) Adiabatic complete combustion

4

2) Uniform water temperature inside the boiler (Tw_{ex})
3) Thermal capacity fully concentrated in water
4) Pre-flush effect neglected
5) Ambient losses on water (through boiler jacket) neglected.This assumption is appropriate for most of the modern boilers.Consequently the only ambient losses are those through combustion chambers windows (thus constant as radiative heat exchange is prevailing), and useful powers on gas and water side are equal for steady-state regime
6) Flow rate and temperature inputs (water, fuel, combustion, air) are constant.Fuel and air temperatures are supposed equal to the reference temperature (25°C).
7) The fast transient evolutions over the first period (Figure 2) are neglected.These influences are to be treated separately when tuning the model.

4.5. Model 1

The boiler is considered as a single cross-flow (gas-water) heat exchanger as shown in figure 3.The inputs are the gas (air + fuel) and water flow rates and supply temperatures.The parameters are the thermal capacity and the fuel LHV . The outputs are gas and water exhaust temperatures.
The useful power injected is calculated on water side in steady-state regime.
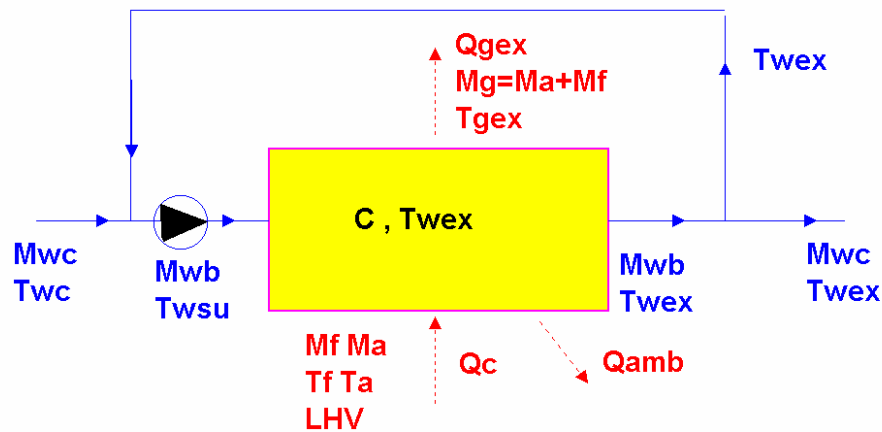

Figure 3. Model 1

4.6.Model 2

The boiler is considered as two gas-water heat exchangers in serie, corresponding to the combustion chamber and boiler heat exchanger respectively. The thermal capacity is also split into two values as calculated hereabove. The models scheme is shown in figure 4. Since there is no intermediary measure on water circuit (Tw$_{ex1}$), the useful power injected in both heat exchangers is calculated on the gas side, using the adiabatic flame temperature and flue gas exhaust temperature.

4.7.Prediction of Water Temperatures Evolution

MODEL 1:

According to the typical assumptions and models structure, one can calculate the steady-state useful power injected in the boiler :

$$\dot{Q}_{inj} = \dot{Q}_{cons} - \dot{Q}_{amb} - \dot{Q}_{chimney} = \dot{M}w_c \ c_w \ (Tw^*_{ex} - Tw_c)$$

(2)

where

$\dot{Q}_{cons}$ 5- is the consumed power

$\dot{Q}_{amb}$ 6- is the ambient loss (through combustion chamber windows)

$\dot{Q}_{chimney}$ 7- is the chimney loss

$\dot{M}w_c$ 8- is the cold water mass flow rate

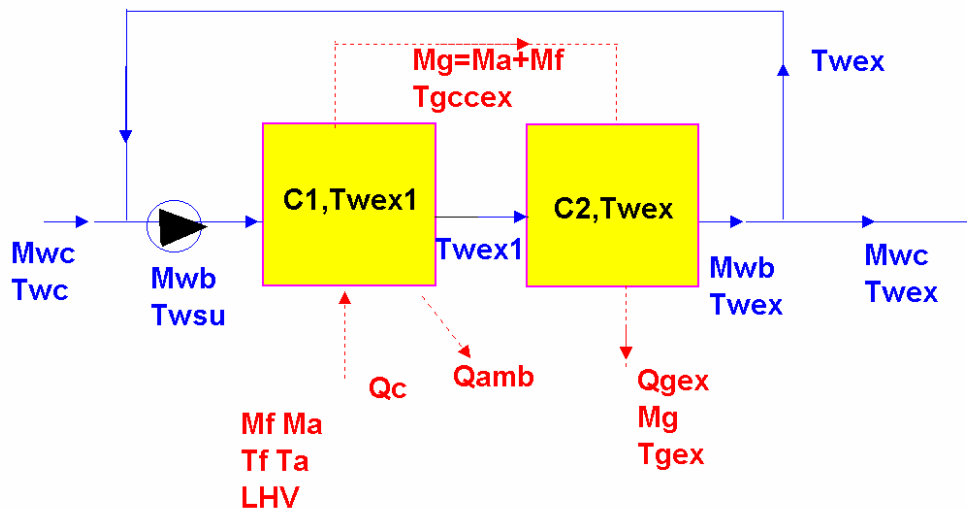Tw^*_{ex} 9- steady-state water exhaust temperature

Figure 4. Model 2

The supply and exhaust water temperatures are calculated using "classical" relationships for energy balance :

$$C_{tot} \frac{dT w_{ex}}{d\tau} + \dot{M} w_c \, c_w \, (T w_{ex} - T w_c) = \dot{Q}_{inj} \tag{3}$$

$$T w_{su} = \frac{R - 1}{R} \, T w_{ex} + \frac{T_{wc}}{R} \tag{4}$$

with

$$R = \frac{T w_{ex}^* - T w_c}{T w_{ex}^* - T w_{su}^*} = \frac{\dot{M} w_b}{\dot{M} w_c} \tag{5}$$

where

$T w_{ex}^*$, $T w_{su}^*$ 13 are the steady-state values.

$\dot{M} w_b$ 14 is the water mass flow rate across the boiler .

From equation (3), the time constant is :

$$\tau_c = \frac{C_{tot}}{\dot{M} w_c \, c_w} \tag{6}$$

MODEL 2:

Using the same assumptions, the useful powers are :
- For the combustion chamber :

$$\dot{Q}_{inj_1} = \dot{M}_g \, (h_{(Tad)} - h_{(Tg_{ccex}^*)}) \left(1 - \frac{A_{win}}{A_{cch}} \right) \tag{7}$$

where:

T_{ad} - adiabatic flame temperature.

Tg_{ccex}^* 17- steady-state flue gas exhaust temperature .

$h_{(Tad)}$, $h_{(Tg_{ccex}^*)}$ 18 - the corresponding enthalpy .

$\dot{M}_g$ 19- flue gas mass flow rate .

A_{win}, A_{cch} - areas of quartz windows and combustion chamber respectively .
Obs. : the calculation is performed supposing that radiative heat transfer is prevailing.
$A_{win} \approx \sim 3 * 10^{-3} \, A_{cch}$
- For the heat exchanger :

$$\dot{Q}_{inj_2} = \dot{M}_g \, (h_{(Tg_{ccex}^*)} - h_{(Tg_{ex}^*)}) \tag{8}$$

with

Tg_{ex}^* 21- chimney flue gas steady-state temperature (°C)
The water temperatures shape is calculated using the next relationship :

7

$$C_1 \frac{d Tw_{ex1}}{d\tau} + \dot{M} w_c \ c_w \ R \ (Tw_{ex1} - Tw_{su}) = \dot{Q}_{inj_1} \tag{9}$$

$$C_2 \frac{d Tw_{ex}}{d\tau} + \dot{M} w_c \ c_w \ R \ (Tw_{ex} - Tw_{ex1}) = \dot{Q}_{inj_2} \tag{10}$$

Tw_{su} 24 is calculated using equation (4)

where $\quad\quad\quad\quad C_1 + C_2 = C_{tot}$ (J/K) $\tag{11}$

Tw_{ex1}- water temperature at the exhaust of combustion chamber (not measured) (°C)

The resulting time constants are : $\quad \tau_{c1} = \dfrac{C_1}{\dot{M} w_c \ c_w} \ ; \ \tau_{c2} = \dfrac{C_2}{\dot{M} w_c \ c_w} 25 \tag{12}$

with : $\quad \tau_{c1} + \tau_{c2} = \tau_c \ 26 \tag{13}$

RESULTS :

A comparison between simulated and measured temperatures shape is presented in figure 5 (for high firing rate).The mean relative error on useful power over is calculated over the stabilization period :

$$\overline{\varepsilon}_w = \frac{100}{n} \sum_{i=1}^{n} \frac{|Tw_{ex(mes)i} - Tw_{ex(mod)i}|}{Tw_{ex(mes)i} - Tw_c} \tag{14}$$

where :

   n - number of steps
   (mes),(mod) - index for measured and model values

The calculated values obtained for the error are :

MODEL1 : 4,17 % (LFR) ; 5,06% (HFR)

MODEL2 : 3,53% (LFR) ; 4,56% (HFR)

Both models are able to reproduce the general shape of water temperatures with an accuracy of 3 ÷ 5 %. The improvements made by using the second model are not significant.

The "delay" between measured and modeled curves is explained by the energy injected in the system during the "dead" time. In fact, by neglecting the transport time on water side, one may overestimate the thermal capacity (underestimation of temperature values).

The lack of accuracy of the models may be decreased by applying corrections based on physical assumptions over the initial period τ_o.
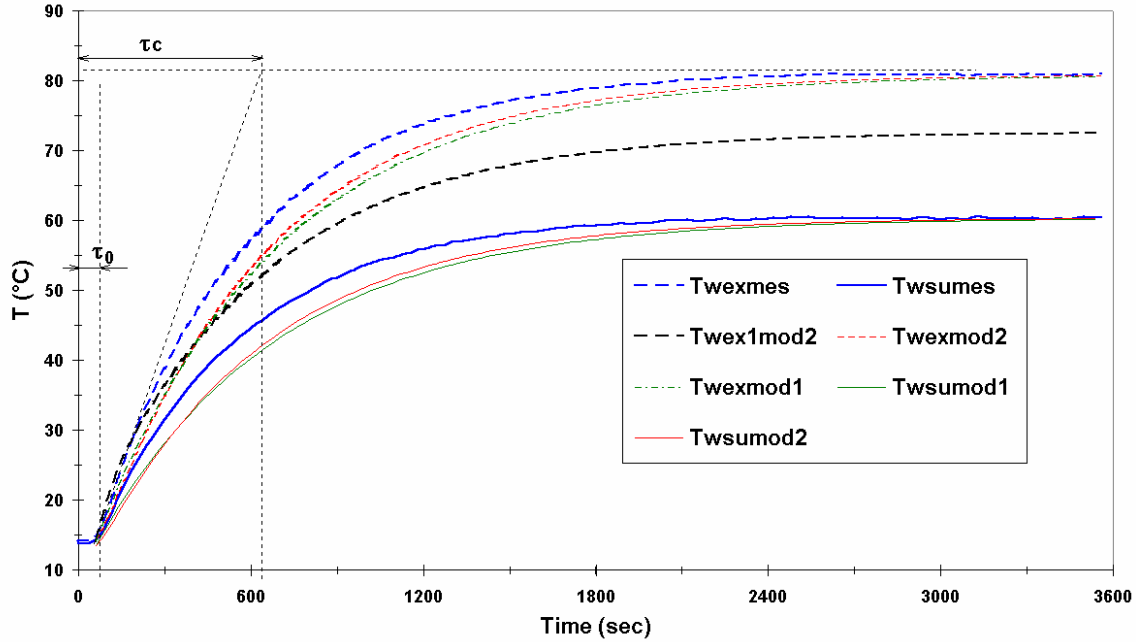
Figure 5. Water temperatures evolution for experimental data, model1 and model 2 (HFR)

MODEL TUNING :

The following hypothesis are assumed :
a.) The "dead" time corresponds to the water transport delay between the combustion chamber exhaust and boiler exhaust (locations X1 and X2 in figure 1) by assuming a plug flow.
b.) The heat released by the flue gas during the dead time, brings a fraction "y" of the thermal capacity at the steady-state level of temperature. Though the dead time is :

$$\tau_o \; = \; \frac{V_{w2} \; \rho_{wo}}{\dot{M} \; w_c \; R}$$

(15)

V_{w2} - is the water volume in heat exchanger (in this particular case, the value is known as explained hereabove).
ρ_{wo} - water volume mass at initial moment (kg/m3).
If neglecting the volume mass variation, the "dead" time will be given as function of the time constant:

$$\tau_o \; = \; \frac{V_{w2} \; \overline{\rho}_w \; c_w}{\dot{M} \; w_c \; c_w \; R} \; = \; \frac{C_2}{C_{tot} \; R} \; \tau_c$$

(16)

The accuracy of the calculation depends on the data acquisition time-step.
However, the assumption is satisfactory as the error produced does not exceed the time step (see figure 6).
The correction coefficient for dead time is $C_{\tau o} = (1 - y)$.

9

For the model 1 :

$$y = \frac{\dot{Q}_{inj}}{Tw_{ex}^* - Tw_c} \frac{\tau_o}{C_{tot}}$$

(17)

For the model 2 :

$$y_1 = \dot{Q}_{inj} \frac{1}{Tw_{ex}^* - Tw_c} \frac{\tau_o}{C_{tot}}$$

(18)

$$y_2 = \dot{Q}_{inj} \frac{2}{Tw_{ex}^* - Tw_c} \frac{\tau_o}{C_{tot}}$$

(19)

The "tuned" value of thermal capacity is thus :
Model 1:

$$C_{cor} = C_{\tau o} \, C_{tot} = (1 - y) \, C_{tot}$$

(20)

Model 2 :

$$C_{cor}1 = C_{\tau o1} \, C_1 = (1 - y_1) \, C_1$$

(21)

$$C_{cor}2 = C_{\tau o2} \, C_2 = (1 - y_2) \, C_2$$

(22)

TUNED MODEL RESULTS

Calculated and experimental temperature shapes for the two models are plotted in figures 7 and 8 for high firing rate. The results show a good agreement (error range of ~ 1 %). It is obvious that both models provide the same accuracy level. The values for ε_w . are :
MODEL 1 : 1,15% (LFR) ; 1,04 (HFR)
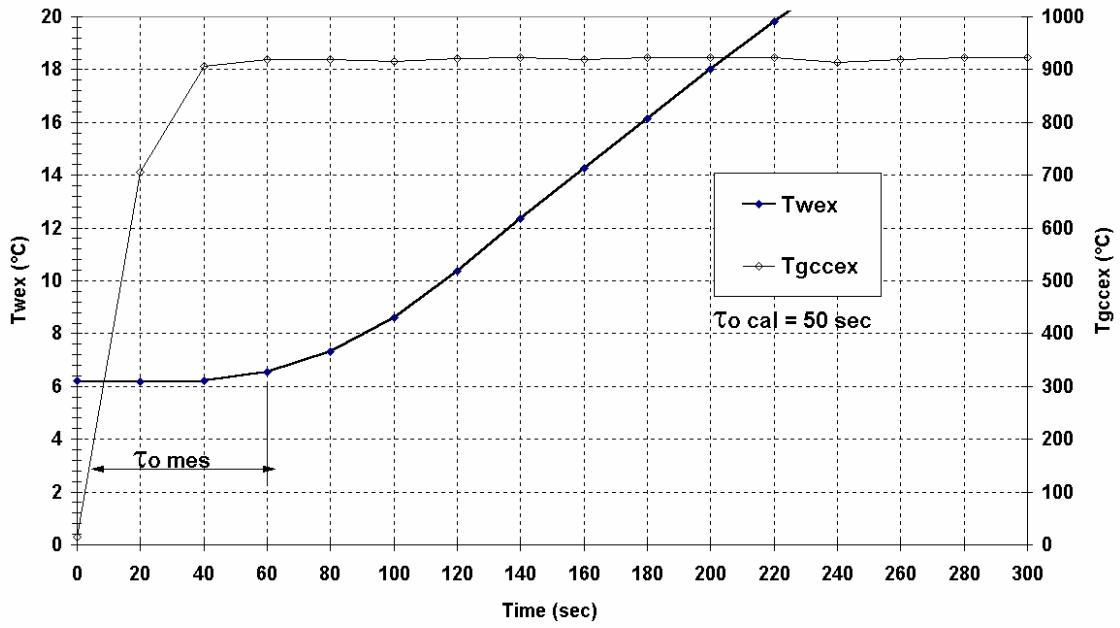MODEL 2 : 1,50 (LFR) ; 0,83 (HFR)

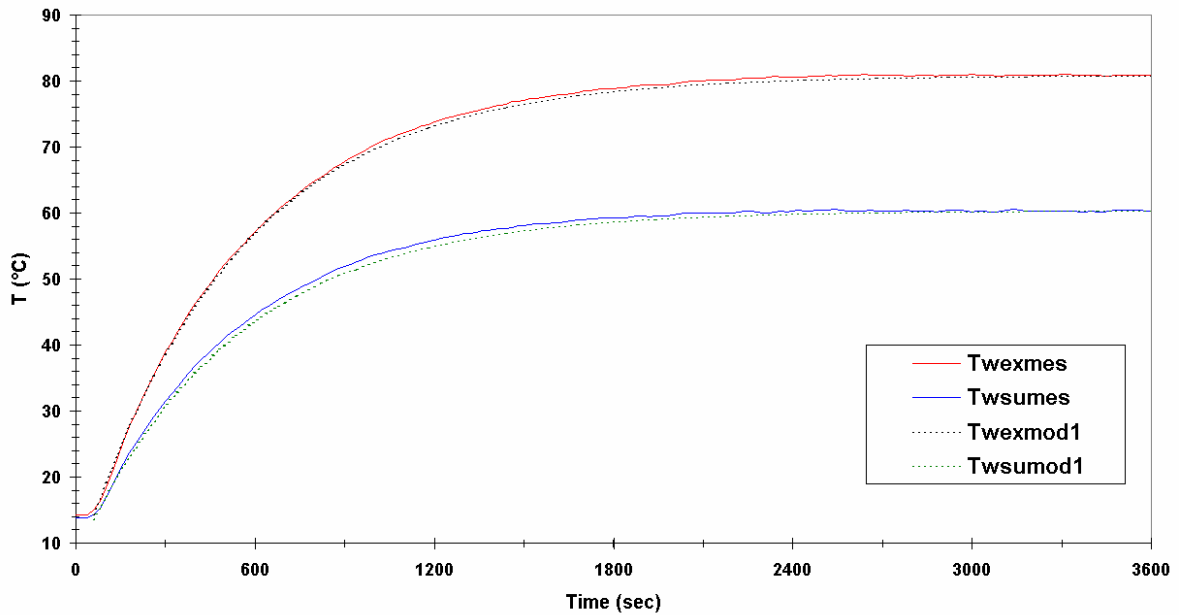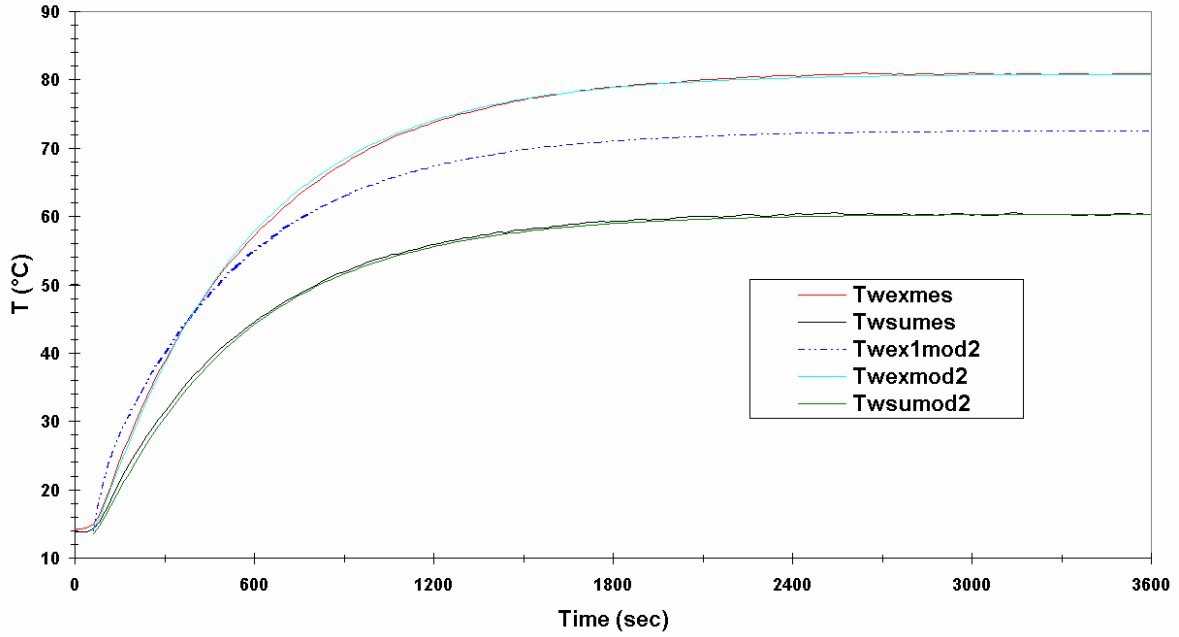**Figure 6**. Typical "start-up" temperature evolutionsl

Figure 7 . Water Temperatures evolution : experimental and "tuned" model 1 values

Figure 8. Water temperatures evolution : experimental and "tuned" model 2 values

4.8. Prediction of Flue Gas Temperature

The problem is the estimation of the flue gas temperature at the chimney, the combustion chamber exhaust temperature being given and supposed constant. According to the previous assumptions (no capacity on flue gas) and using the second model, it appears that (eq.8):

$$h_{(Tg_{ex})} = \frac{-\dot{Q}_{inj2}}{\dot{M}_g} + h_{(Tg^*_{ccex})} = ct \tag{23}$$

Which is equivalent to

$$Tg_{ex} \stackrel{=}{\underset{ct}{}} ct \;(!) \tag{24}$$

On the other hand, if using the <u>measured value</u> for the combustion chamber exhaust temperature Tg_{ccex} :

$$Tg_{ex} = Tg_{ccex} - \frac{\dot{Q}_{inj2}}{\dot{M}_g \; \bar{c}_{pg}} \tag{25}$$

with

$$\bar{c}_{pg} = c_{pg} \left(\frac{Tg_{ccex} + Tg_{ex}}{2} \right)$$

(26)

The results plotted in figure 9 (using eq. 24) are neither satisfactory. <u>It appears that chimney gas temperature can not be simulated when neglecting the thermal capacity on gas</u>. Moreover, this fact may be put in evidence using figure 10 and the model assumptions. Since

the water temperatures are matching (as shown hereabove - chapter 4.7), we assume that the thermal capacity on water side is proportional to the area (1) in figure 10 (assumption of equal and constant useful powers on water and gas). Consequently, the remaining area (2) represents the real thermal capacity on flue gas side.

It appears that an accurate method of modelling transient behaviour is splitting the thermal capacity between water and flue gas (Lebrun et al., 1985).
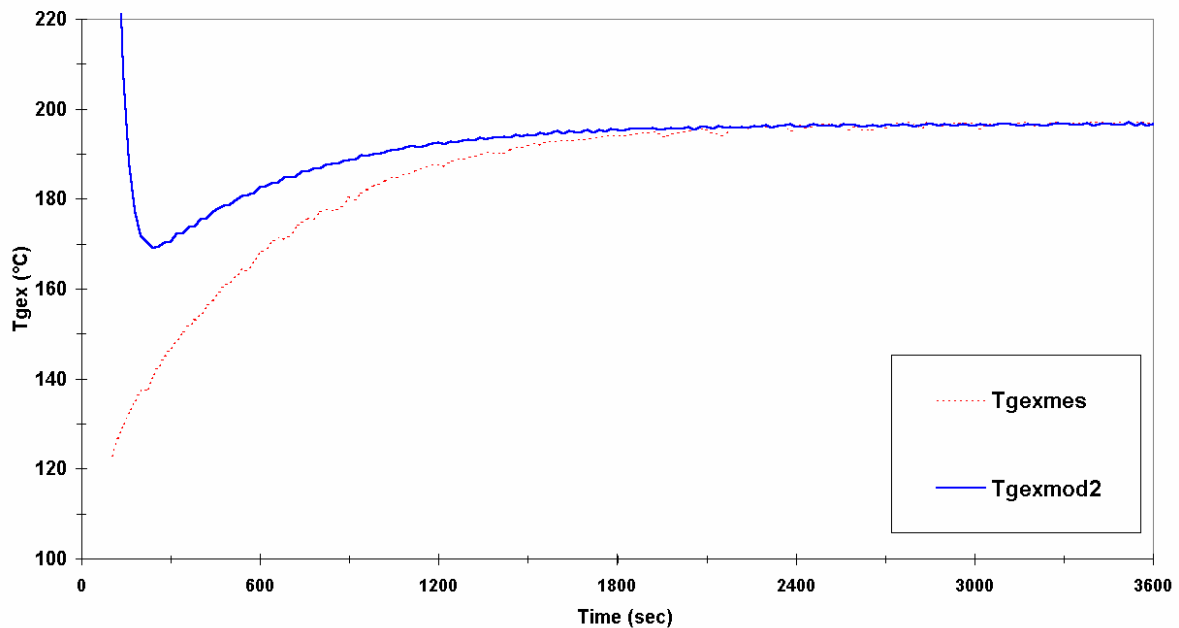
Figure 9. Measured and predicted chimney flue gas temperatures evolution. Thermal capacity on flue gas neglected
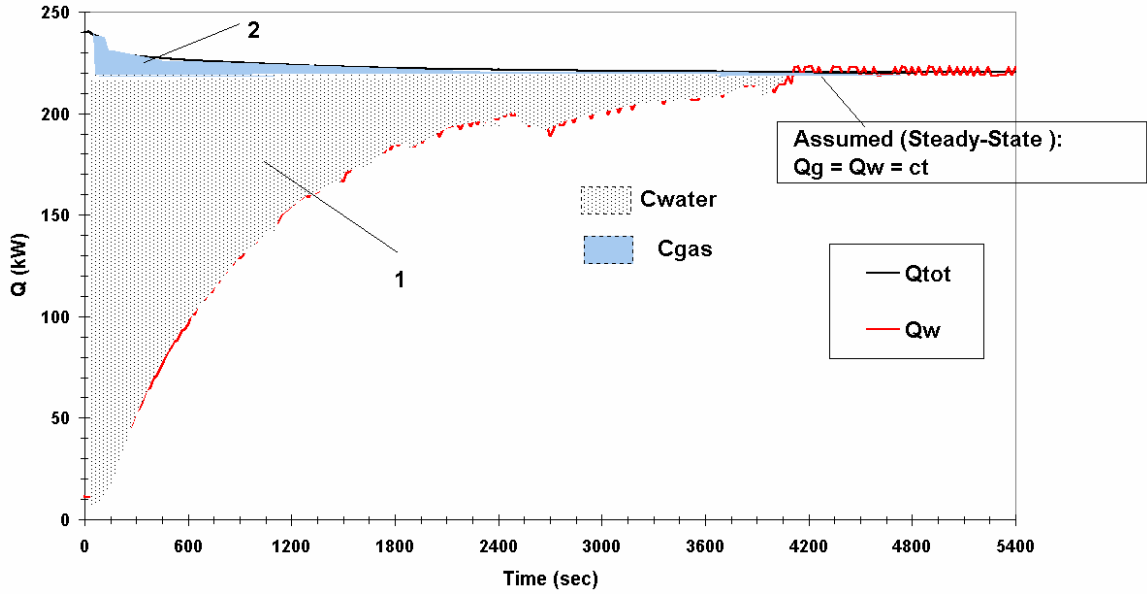
Figure 10. Evolution of total and useful power of the boiler

4.9. "Split" Capacity Assumptions - Second Modelling Case

The total thermal capacity is divided as follows :

$$C_{tot} = C_{water} + C_{gas} = (1 - X) . C_{tot} + X . C_{tot}$$

(27)

a.) The other assumptions (first case) are maintained.

b.) The new hypothesis is applied to the model 2.

c.) The fraction "X" of the thermal capacity includes the mass of <u>flue gas tubes</u> contained in the heat exchanger.For the combustion chamber, the thermal capacity is still fully concentrated in water.

Notice that in many practical cases, such details on boilers structure may not be available (tube dimensions).Consequently the capacity fraction "X" is to be deduced using an experimental fit.

However, these new assumptions give a <u>physical interpretation of the phenomena as the tubes temperature is closer related to the flue gas temperature shape, while in the combustion chamber the energy transfer is practically instantaneous (at the time scale)</u>.

d.) The "dead" time correction for the second capacity (heat exchanger) is made on the flue gas side.It is assumed that during the "dead" time, all the flue gas heat is released in the metal tubes (during this period, chimney losses are assumed null $Tg_{ex} = Tg_{ex0}$).

$$y_2 = \frac{\dot{Q}_{inj2}}{Tg_{ex}^* - Tg_{ex0}} . \frac{\tau_o}{C_{tot}}$$

(28)

14

with Tg_{ex0} = the initial (pre-flush) chimney gas temperature .

4.10. Prediction of Water Temperature Shapes - "Split" Capacity Model

The compared shapes and synthesis values using the "split" assumptions and <u>model 2</u> are given in figure 11 (HFR example) . The thermal capacities used are :

$$C_{cor1} = (1 - y_1) \, C_1 \tag{29}$$

$$C_{cor2} = (1 - X) \, C_2 \tag{30}$$

where : $X \, C_2 = m_{tubes} \, C_{metal} \approx 395 \, kg * 500 \, J/kg \, K \approx 0{,}197 * 10^6 \, J/K$

There is practically no difference with the previous results (ε_w):

MODEL 2 : 1,45% (LFR) ; 0,81% (HFR)

4.11.Prediction of Flue Gas Temperature Shape - Split Capacity Model

The energy balance on flue gas is :

$$X \, C_2 \, (1 - y_2) \, \frac{d \, Tg_{ex}}{d\tau} + \dot{Q}_{inj\,2} = \dot{M}_g \, \bar{c}_{pg} \, (Tg_{ccex}^* - Tg_{ex}) \tag{31}$$

The experimental and simulated curves plotted in figure 12 show a fully satisfactory accuracy as the mean relative error on flue gas side (equation 32) is : 0,13% (LFR) ; 0,10% (HFR)

$$\bar{\varepsilon}_g = \frac{100}{n} \, \sum_{i=1}^{n} \frac{| \, Tg_{ex(mes)} - Tg_{ex(\,mod\,)} \, |}{\left(Tg_{ccex}^* - Tg_{ex(mes)} \right)} \tag{32}$$
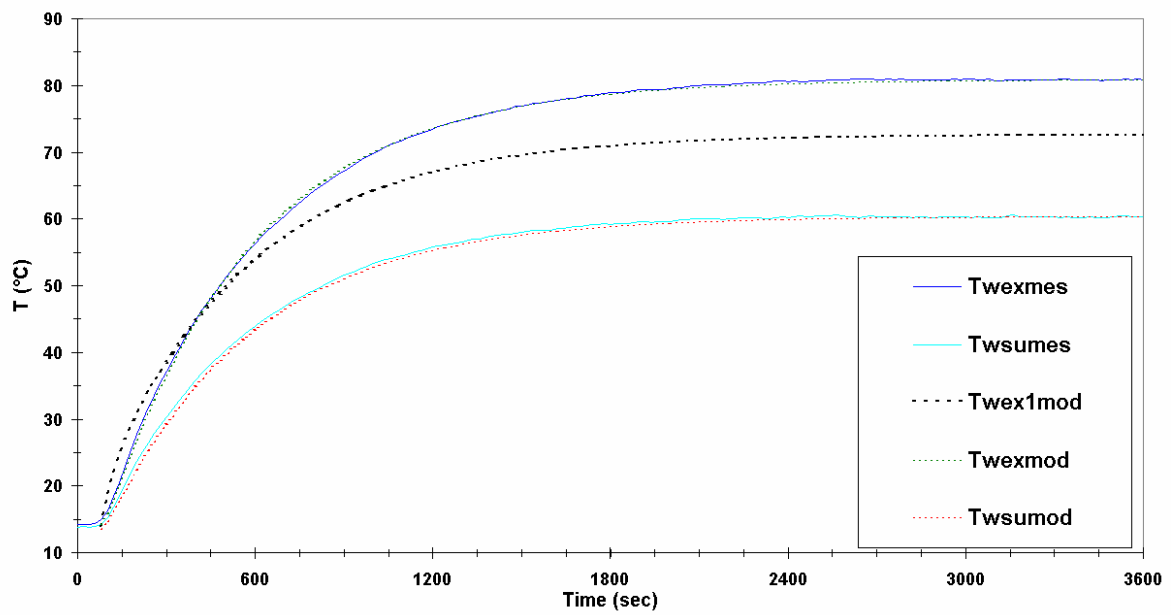
Figure 11. Evolution of measured and predicted water temperatures using model 2 and a "split" thermal capacity (water & flue gas)
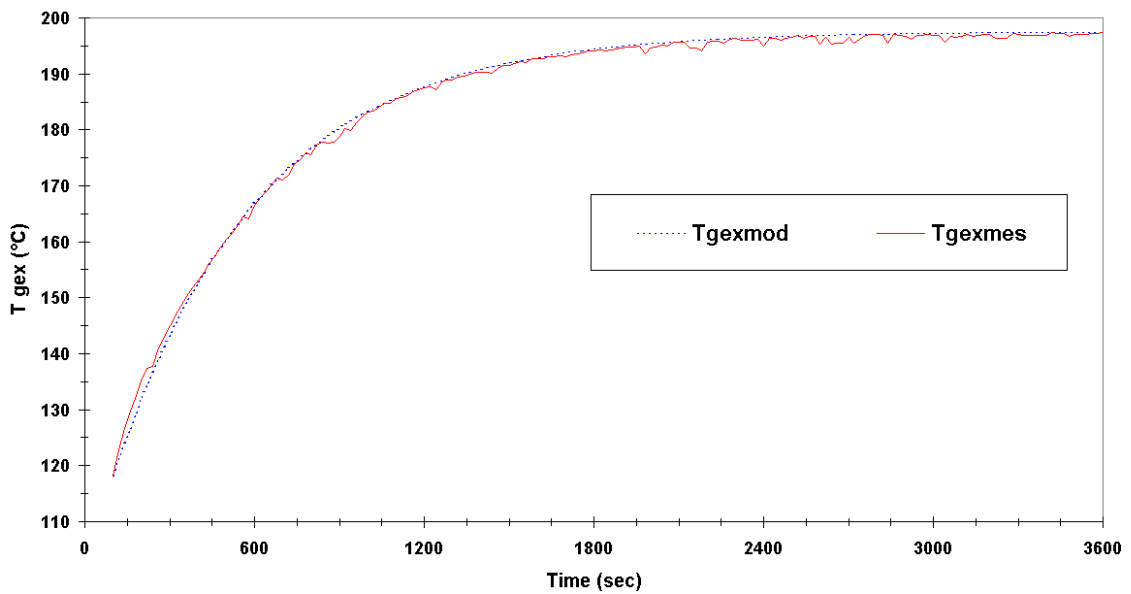
Figure 12. Evolutions of measured and predicted flue gas temperatures using model 2 and a "split" thermal capacity (flue gas & water)

16

5.SIMULATION OF "COOL-DOWN" REGIME (OFF period)

5.1.Experimental Results

The typical temperatures evolution over a cool-down regime is shown in figure 13. It appears there is a delay between burner cut-off and damper shut-down.
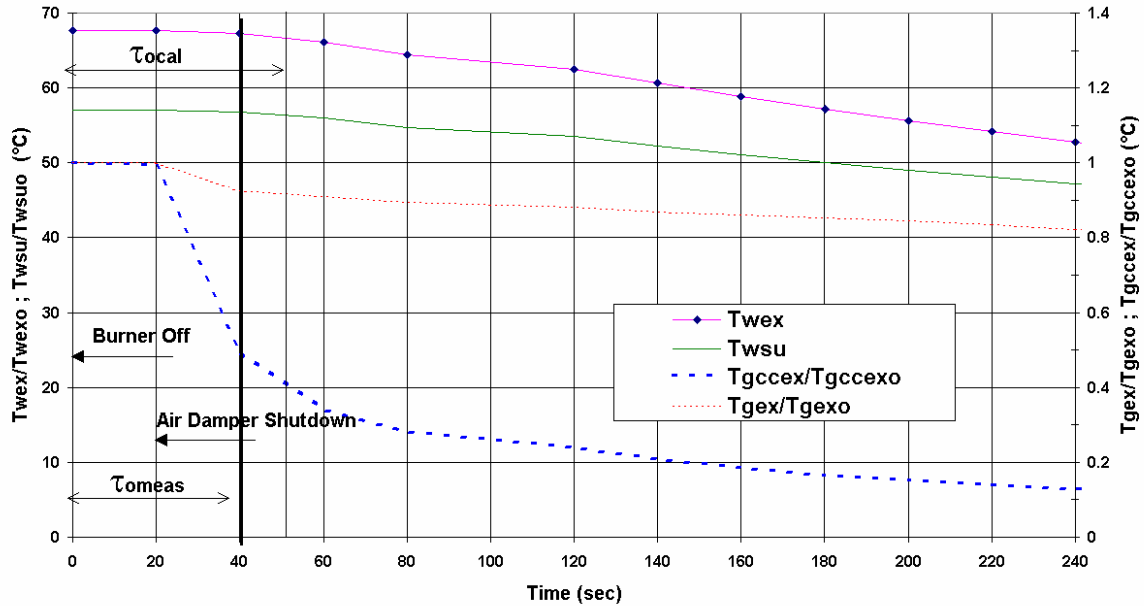

Figure 13. Typical temperatures evolution for "cool-down" regime

5.2.Typical Assumptions

a.) Over the "off" period, the draft air flow rate is negligible (the burner damper is closed).
b.) The cold water flow rate and temperature are assumed constant.
c.) The thermal capacity on flue gas side is fully concentrated in the heat exchanger.
d.) Initial temperature of the metal tubes is supposed equal to the temperature at the chimney exhaust (on air).Thus, there are two capacities with two initial temperatures that are releasing the heat to the water flow.
d.) The initial time chosen for simulation is :
with: τ_{OFF} = burners cut-off moment . $\tau_{coolO} = \tau_{OFF} + \tau_O$ (33)
τ_o = "dead" time.
In this case, the correction for the "dead" time delay is useless as there is no injected power.
e.) The fast transient evolutions on the gas side during the "dead" time are neglected.

5.3.Prediction of Water Temperatures Shape

The model used is the first order model (Model 1) with the thermal capacity split between flue gas and water . The water temperature evolution is calculated using the energy balance:

$$X\ C_2\ \frac{d\,Tg_{ex}}{d\tau}\ +\ (\ C_1\ +\ (1\ -\ X)\ C_2\ )\ \frac{d\,Tw_{ex}}{d\tau}\ =\ -\ \dot{M}\ w_c\ c_w\ (\,Tw_{ex}\ -\ Tw_c\,) \tag{34}$$

$$-\ X\ C_2\ \frac{d\,Tg_{ex}}{d\tau}\ =\ AU_{g\text{-}w}\ \Delta t_{\ln\ g\text{-}w} \tag{35}$$

Tw_{su} 49 is calculated using equation (4).

where : $AU_{g\text{-}w}$ is the global heat transfer coefficient between gas tubes and water .

$\Delta t_{\ln\ g\text{-}w}$ is the mean logarithmic temperature difference .

The AU mean value is calculated using the experimental flue gas, and water temperature shapes.

Results obtained thanks to equations (34) and (35) are compared with experimental data of one "cool-down" test in low firing rate, and presented in figures 14 and 15.Notice that due to the small temperature differences on water, the relative error defined by equation (14) is no longer relevant. Thus the error is calculated on the global energy released to the water over the cooling period :

$$\overline{\varepsilon}_{wcool}\ =\ \frac{\left|\ \sum_{i=1}^{n}\ (\,Tw_{ex\ mod}\ -\ Tw_c\,)\ -\ \sum_{i=1}^{n}\ (\,Tw_{ex\ mes}\ -\ Tw_c\,)\ \right|}{\sum_{i=1}^{n}\ (\,Tw_{ex\ mes}\ -\ Tw_c\,)}\ .\ 100 \tag{36}$$

The error on the gas (air) side is still calculated by means of equation (32) .The results obtained are : ε_{wcool} = 3,47% ; ε_g = 20,84%.

The general shape of water temperature is reproduced with a good accuracy while there is a big error on the air (gas tubes) temperature.
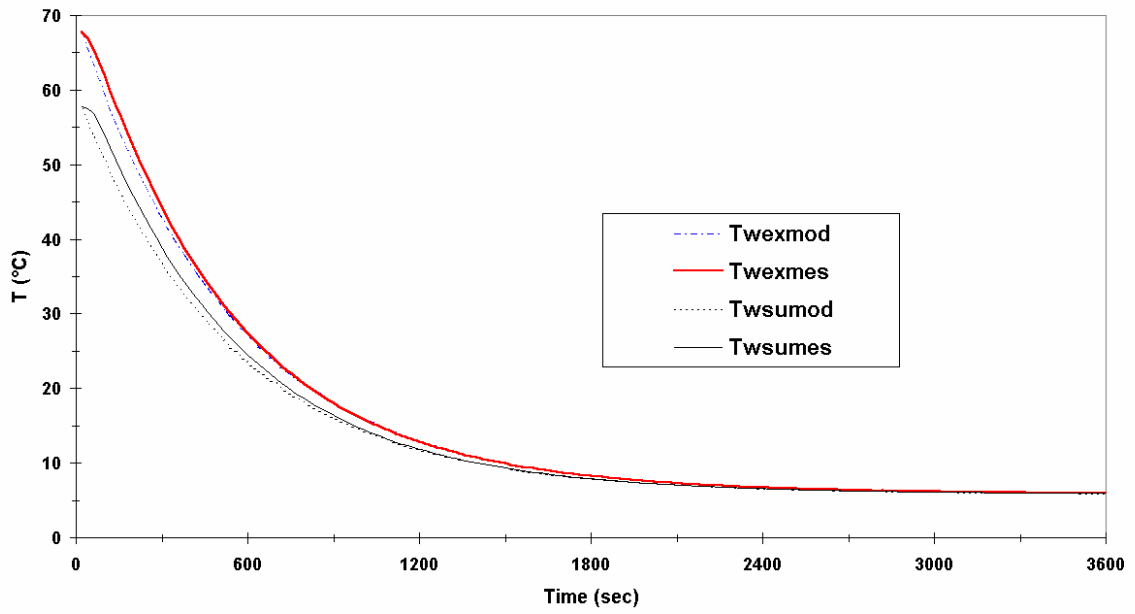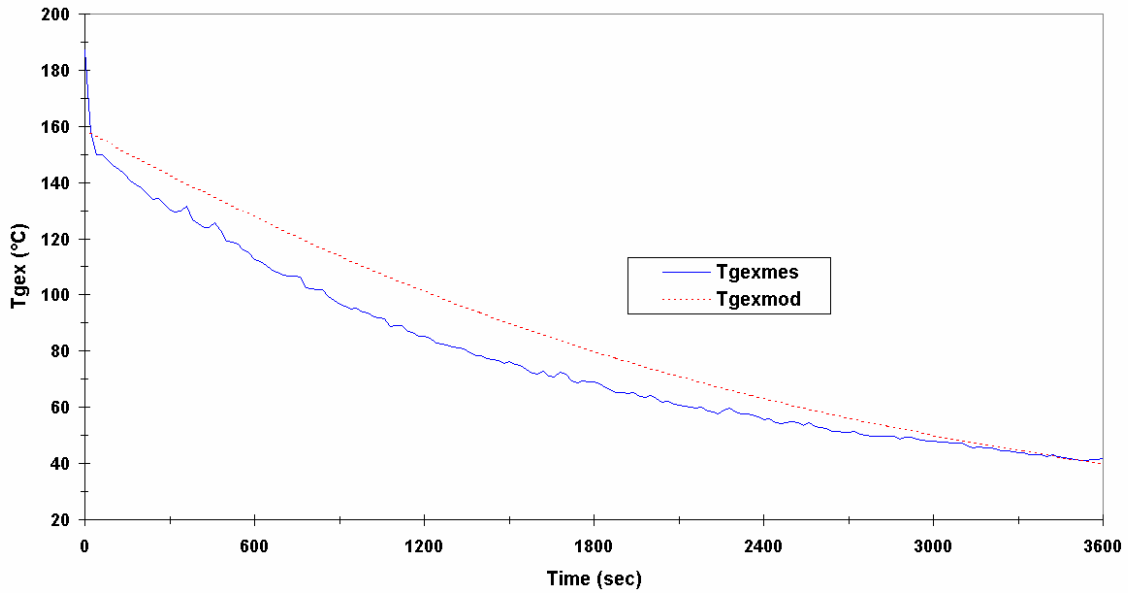
Figure 14. Measured and predicted water temperatures evolutions for "cool-down" regime using model 1 and a "split" thermal capacity. Air draft influence is neglected.

Figure 15. Measured and predicted flue gas temperature evolutions for "cool-down" regime using model 1 and "split" thermal capacity. Air draft influence is neglected.

If trying to model the flue gas temperature evolution one is obliged to take into account the air draft influence.

It is assumed that air flow rate inside chimney and boiler is only due to natural convection. A mean pressure drop per unit length along the flue gas circuit is calculated using the parameters for nominal steady-state foperating conditions (high firing rate and 0,1 air excess):

$$\lambda = \frac{2 \, \Delta p \, Dm}{l \, v^2 \, \rho_n} \quad (Pa \, / \, m)$$

(37)

where : Δp is the total pressure drop in nominal conditions - 200 Pa (producer data).

Dm is the mean equivalent diameter along the circuit .

ρ_m is the mean gas volume mass during functioning period .

l is the total length of gas circuit .

v_m is the mean gas velocity across the circuit .

(38)

$$v_m^2 = \frac{4 \, \dot{M}_g^2}{\pi \, Dm^4 \, \rho_m^2}$$

$\dot{M}_g$ 53is the flue gas mass flow rate in nominal conditions (ON period)

The air draft velocity is calculated as :

$$v_D = \sqrt{\frac{2 \Delta \, p_d}{\lambda \, l} \, \frac{Dm}{2}}$$

(39)

where: Δp_d is the pressure difference due to temperature .

$$\Delta \, p_d = g \, h \, (\rho_{ref} - \rho_D)$$

(40)

20

where :h is the chimney height.

ρ_{ref} is the air volume mass at reference temperature .

ρ_D is the air draft volume mass at gas exhaust temperature $(\rho_D=\rho_D (Tg_{ex}))$.

The air draft mass flow rate is :

$$\dot{M}_{ad} = Am\ V_D\ \rho_D \tag{41}$$

where Am is the mean cross section through gas circuit .

For the studied example, one will obtain :

$$\dot{M}_{ad} \equiv 0,16 \sqrt{(\rho_{ref} - \rho_D)\ \rho_D} \tag{42}$$

In order to predict air draft and water temperatures evolution, it is assumed that the heat accumulated in the gas tubes is released on one side to the water flow and on the other to the air draft flow. Consequently, the following equations are used :

$$X C_2\ \frac{dTg_{ex}}{d\tau} + (C_1 - (1 - X)C_2)\ \frac{dTw_{ex}}{d\tau} = -\dot{M} w_c\ c_w\ (Tw_{ex} - Tw_c) \tag{43}$$

$$- XC_2\ \frac{dTg_{ex}}{d\tau} = \overline{AU}^*_{g\text{-}w}\ \Delta t_{\ln g\text{-}w} + \dot{M}_{ad}\ c_{ad}\ (T g_{ex} - T_{ref}) \tag{44}$$

$T w_{su} 60$ is calculated using equation (4).

The new value of the global heat transfer coefficient AU*g-w is deduced using the experimental evolution of temperatures (numerical fit).The flue gas temperature evolution is plotted in figure16.
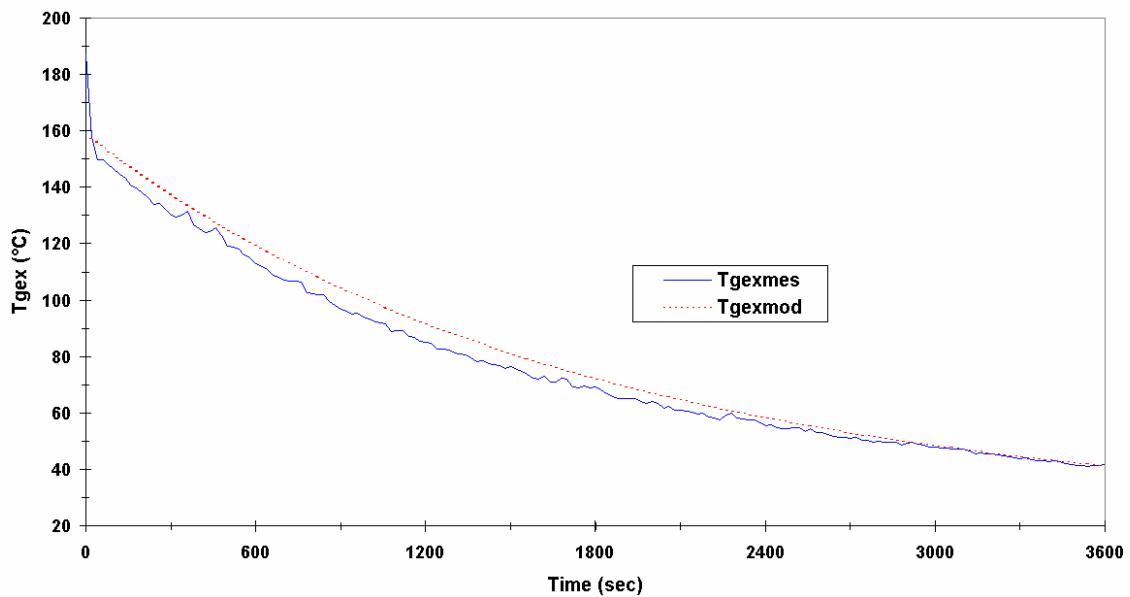
Figure 16. Improvements on case of figure 15 when taking into account the air draft

The corresponding accuracy when using these new assumptions is :
$\varepsilon_{wcool} = 2,87\% \; ; \varepsilon_g = 8,19\%$.

Major improvements are made on air draft temperature prediction, thus this model is regarded as a first approach on a non-homogeneous cool-down evolution.It is obvious that the air draft influence strongly depends on the initial flue gas temperature and on the external climate.

6.   CONCLUSIONS

The first order model (1) is able to reproduce transient <u>water temperatures</u> evolution for the "heat-up" regime using constant inputs and system parameters (producer data).No significant improvements are observed when using the two-exchanger model (2). As the assumptions do not require detailed knowledge on boilers design, it is appropriate for developing a general model.In the case of the "cool-down" regime the model development requires experimental results in order to calculate the gas-water heat transfer coefficient.

If dealing with flue gas (or air draft) temperatures, the use of model 2 is compulsory. It also requires detailed producer data (the thermal capacity is assumed as split between water and flue gas) and access to special measuring locations (combustion chamber exhaust).This kind of model provides accurate temperature prediction but has a limited range of application.

Major difficulties in models tuning are given by flue gas fast transient regimes and water transport delay (start-up and cut-off moments).In this case, simple corrections based on physical assumptions are successful. A higher accuracy may be obtained if "zooming" on time period (decreasing the measure time step).

22

The results presented in this work must be extrapolated with care until they are validated on other examples.

7.   REFERENCES

- AST H., STEPHAN W. Report on the exercice 1A on the La Chaumiere building " Simulation of the heating plant ". International Energy Agency, Annex 10 - System Simulation, 1983.
- BOURDOUXHE J-P., LEBRUN J. Reference Guide for Dynamic Models of HVAC Equipment - ASHRAE Project 1996;
- CHI J., CHERN L., DIDION D.A., A commercial heating boiler transient analysis simulation model (DEPAB2) NBSIR 83-2638, National Bureau of Standards, Washington D.C., 1983.
- CLAUS G., STEPHAN W. A general computer simulation model for furnaces and boilers. ASHRAE Transactions, Vol 91, Part 1, 1985.
- KREITH F. Principles of Heat Transfer - Harper International Edition - 1973.
- LEBRUN J., HANNAY J., DOLS J-M. Research of a Good Boiler Model for HVAC Energy Simulation, ASHRAE Transactions, 1985.
- PARK C., KELLY G., A study on the performance of residential boiler for space and domestic hot water heating. National Institute of Standards and Technology, USA, NISTIR-89-4104, 1989.
- ****** - ASHRAE Handbook - Fundamentals, 1993.

SYMBOLS (*)

A - surface

AU - global heat transfer coefficient
C - thermal capacity
c - specific heat
D - diameter
h - enthalpy
LHV - low heating value
$\dot{M}$ 61 - mass flow rate

$\dot{Q}$ 62 - heat flow rate
Δp - pressure drop
T - temperature
Δt - temperature difference
V - volume

SUBSCRIPTS

a   - combustion air

ad - air draft
b   - boiler
c   - cold
cc   - combustion chamber
ex - exhaust
f   - fuel
g   - flue gas
inj - "injected" power
m   - mean value
o   - initial time (value)
su - supply
tot   - total value

v - velocity
ε - relative error
λ - pressure drop per unit length
ρ - volume mass
τ_c - time constant
τ_s - stabilization time
τ_o - "dead" time

w   - water
cor - corrected value
ref   - reference value
mes - measured values
mod - predicted values
cons - consumed power
amb - ambient loss

(*) - SI units are used through all the text

SUPERSCRIPTS

*   - steady-state value